

Automatic Detection of Water Surfaces Using K-means++ Clustering Algorithm with Landsat-9 and Sentinel-2 Images on the Google Earth Engine Platform

Osman Salih Yilmaz*¹

Abstract: Water is the most essential requirement for sustaining the life cycle on Earth. These resources are constantly dynamic due to anthropogenic and climatological effects. Therefore, management and consistent water policies are necessary to be followed for the proper management of water resources. Monitoring water resources is possible by accurately determining the water surface boundaries and determining the change in water surface areas. In this context, the normalized difference water index (NDWI) and modified normalized difference water index (MNDWI) were computed using JavaScript on the Google Earth Engine (GEE) through Landsat-9 and Sentinel-2 satellite images. Water pixels were extracted from other details using the K-means++ cluster algorithm based on the calculated indices. The water surfaces were determined using the Otsu thresholding method, which is the most preferred method for the NDWI and MNDWI indices calculated from the Sentinel images and was used as verification data. The K-means++ clustering algorithm yielded successful results in detecting water surfaces. In the two indices used, the NDWI index was found to be more successful than the MNDWI index. For Landsat-9 images, OA, Kappa, and F1-scores in the NDWI index were calculated as 99.72%, 0.994, and 99.57%, respectively. The overall accuracy (OA), Kappa, and F1-scores in the NDWI index for Sentinel-2 images were calculated as 99.39%, 0.986, and 99.04%, respectively. This study demonstrated that clustering algorithms can be successfully applied to automatically detect water surfaces.

Keywords: Remote sensing, Google Earth Engine, NDWI, MNDWI, K-means++, Terkos Lake.

¹Address: Manisa Celal Bayar University, Demirci Vocational School, 45900, Manisa, Türkiye.

***Corresponding author:** osmansalih.yilmaz@cbu.edu.tr

Citation: Yilmaz, O., S. (2023). Automatic detection of water surfaces using K-means++ clustering algorithm with Landsat-9 and Sentinel-2 images on the Google Earth Engine Platform. Bilge International Journal of Science and Technology Research, 7(2): 95-111.

1. INTRODUCTION

Detection of water surfaces is very important for hydrological processes and the ecosystem. It has become a necessity to monitor water resources that are under pressure due to climatic and anthropogenic effects (Hu et al., 2022). The extensive spread and continuous dynamics of surface waters make their monitoring difficult (Gao et al., 2012; Yilmaz et al., 2023). Nowadays, remote sensing (RS)-based approaches have been very practical in determining water surfaces (Khalid et al., 2021). Various spectral information recorded by satellites provides valuable information about the Earth's surface and water resources (Govender et al., 2007). Synthetic aperture radar (SAR), advanced very high-resolution radiometer (AVHRR), moderate resolution

imaging spectroradiometer (MODIS), and other optical image data are widely used for the detection of water surfaces. In recent years, the processing challenges associated with SAR images and the high cost of high-resolution optical imagery have made Landsat and Sentinel satellites unique resources for the detection and monitoring of surface waters, primarily due to their high temporal, spatial, and spectral resolutions (Cordeiro et al., 2021; Yilmaz et al., 2023). Furthermore, cloud computing systems have eliminated the data storage problem and facilitated the processing and storage of large volumes of satellite images, particularly in recent years. In this regard, Google Earth Engine (GEE), an RS platform, is very useful due to its simultaneous access to many free satellite platforms and its

ability to analyze large volumes of data (Nguyen et al., 2019; Pekel et al., 2016).

The physical properties of the environment surrounding water surfaces and the chemical properties of water cause changes in the electromagnetic spectrum (Elachi and Van Zyl, 2021). Therefore, various methods have been developed to extract water surfaces from other details. Supervised classification (Mahdianpari et al., 2017; Mansaray et al., 2019), unsupervised classification (Gao et al., 2012; S. Reis and Yilmaz, 2008; Zhang et al., 2018), spectral mixture analysis (SMA) (Feng et al., 2016), sub-pixel classification (Liu et al., 2020), water indices (Gao, 1996; Ji et al., 2009; McFeeters, 2013; Qiao et al., 2012; Yang et al., 2017), and clustering algorithms (Cordeiro et al., 2021) are the most commonly used radar and optical-based systems for detecting water surfaces. Each method used to determine water surfaces has its own advantages and disadvantages. Generally, classification techniques require user experience, but spectral indices are independent of user experience and can be used to differentiate water surfaces from other details. Various indices have been developed that aim to enhance water surfaces and suppress other details by utilizing the responses of bands to water and other details in the studies conducted.

The Normalized Difference Water Index (NDWI) suppresses terrestrial plant and soil properties while maximizing the reflection of water surface by using green and near-infrared (NIR) bands (McFeeters, 1996). In urban areas, the modified NDWI (MNDWI) has been proposed using the shortwave infrared (SWIR) band rather than the NIR band for calculating water surfaces (Xu, 2006). To minimize the mixing of water pixels with other pixels in shaded areas and shallow waters, the automatic water extraction indices (AWEI) has been proposed (Feyisa vd. 2014). The AWEI index is designed in two different forms: AWEI_{sh} for shaded areas and AWEI_{nsh} for non-shaded areas. In the resulting indices, each pixel has a gray value. Various thresholding methods are used to extract water surfaces from other details using these gray values. Some of these methods are manual thresholding, while others are automatic thresholding methods such as Otsu's and Canny edge detection (Donchyts et al., 2016; Gu et al., 2021; Rad et al., 2021).

There are various studies available for the detection of water surfaces. Tang et al. (2022) designed an adapted RF algorithm on the GEE platform using Landsat-7 (ETM+), Landsat-8 (OLI), and Sentinel-1 SAR images to detect water surfaces in the study area. The method achieved a water surface detection accuracy of 96.6% and a Kappa statistic of 0.931. Owusu (2022) developed the PyGEE-SWToolbox on the GEE platform and used Landsat, Sentinel-1, and Sentinel-2 images to detect water surfaces in Elephant Butte Lake, Hubbard Creek Reservoir, Clearwater Lake, and Neversink Reservoir in the United States. They utilized NDWI, MNDWI, AWEI, and dynamic surface water extend (DSWE) indices. The time series of water surface areas generated by PyGEE-SWToolbox yielded good results, with R² values ranging between 0.63 and 0.99 for Elephant Butte Lake, Hubbard Creek Reservoir, and Clearwater Lake, except for Neversink Reservoir, which had a maximum R² value of 0.52. Yilmaz (2023) examined the surface water

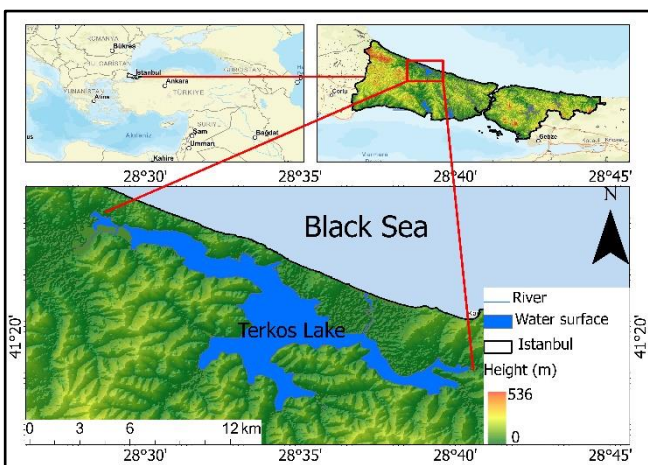
dynamics of lakes in the Lakes Region of Türkiye on the GEE platform from 1985 to 2022. Acigol, Aksehir, Beysehir, Burdur, Egirdir, Ilgin, Isikli, Karatas, Salda, and Yarisli lakes were analyzed using the NDWI index and the Otsu threshold method. Additionally, climate variables were used to analyze the changes in lake surfaces using the Mann-Kendall (MK) and Sen's slope statistical methods. The study found a decreasing trend in the surface areas of all lakes except Acigol. Cordeiro et al. (2021) proposed a machine learning approach for water extraction from a single image using optical high-resolution images that can be applied at a large scale. They utilized random subsampling and a Naïve Bayes classifier for generalization. Unlike other thresholding approaches that only use a single dimension, such as a water index, the proposed method aimed to analyze the applicability of combining different water indices and spectral bands within an unsupervised multidimensional hierarchical clustering. The study was conducted using Sentinel-2 images for 15 different water surfaces in France. They tested combinations of NDWI, MNDWI, Multi-band Water Index (MBWI), B8, and B12 bands and determined that the best two combinations were NDWI and B12. This study is highly valuable in terms of utilizing clustering algorithms for water surface detection. However, despite the various approaches used to identify water surfaces, studies related to clustering algorithms have not gained popularity (Cordeiro et al., 2021).

Therefore, the goal of this study is to detect water surfaces from water extraction indices calculated on optical images using a clustering algorithm instead of thresholding methods, which is different from other studies. For this purpose, NDWI and MNDWI were computed using Landsat-9 and Sentinel-2 images on the GEE platform. Water surfaces were determined using K-means++ clustering algorithm from the calculated NDWI and MNDWI indices. This study is quite valuable in understanding the success of clustering algorithms in determining water surfaces.

2. MATERIAL AND METHOD

2.1. Study Area

Terkos Lake, also called Duru Lake, is located within the boundaries of the Catalca district in the northern part of Istanbul. The lake, which has a coastline to the Black Sea, is situated between the Karaburun and Ormanlı regions (Bayram et al., 2013). Terkos Lake is approximately 40-50 km away from the city and has a surface area of approximately 25 km² (Kaya et al., 2019). With a water potential of 142,000,000 m³/year, Terkos Lake constitutes 30% of the freshwater reserves around Istanbul (Maktav et al., 2002). The location map of Terkos Lake, which is the subject of this study, is presented in Figure 1.

**Figure 1.** Study area

2.2. Data Used

In this study, images captured by Landsat-9's Operational Terrain Imager (OLI-2) and Sentinel-2's Multispectral Instrument (MSI) were used. Landsat-9 was jointly launched by the United States Geological Survey (USGS) and the National Aeronautics and Space Administration (NASA) on September 27, 2021, and operates at an altitude of 705 km. The satellite provides data with a spatial resolution of 30 m, a temporal resolution of 16 days, and a 14-bit radiometric resolution. The OLI-2 sensor captures multi-band images in the visible and mid-infrared wavelengths, and the Thermal Infrared Sensor (TIRS-2) spectrometer analyses ground temperatures. The satellite also improves its ability to detect changes in dark surfaces such as water and dense forests. (Bouslihim et al., 2022). In this study, Landsat-9 Collection 2 Tier 1 top-of-atmosphere (TOA) reflectance calibrated images were used in the GEE platform.

The Sentinel-2 satellites, which are a component of the European Commission's (EC) Copernicus program, consist of two groups, Sentinel-2A and Sentinel-2B. These satellites were launched on June 23, 2015, and March 7, 2017, respectively. They orbit at an altitude of roughly 786 km and provide a combined temporal resolution of 5 days. The MultiSpectral Instrument (MSI) has 13 spectral bands ranging from 10 to 60 m with a 12-bit radiometric resolution. In this research, Sentinel-2 level (L2A) images, which are calibrated for bottom-of-atmosphere (BOA) reflectance, were obtained from the GEE platform.

Spectral band information and resolutions of these images are given in Table 1.

Table 1. Features of Satellite Images (L9/S2A/S2B)

Spectral range	Wavelength	Spatial resolution
Blue (B2)	450-510/496.6/492.1	30/10
Green (B3)	530-590/560/559	30/10
Red (B4)	640-670/664.5/665	30/10
NIR (B5/B8)	850-880/835.1/833	30/10
SWIR-1 (B6/B11)	1,570-1,650/1,613.7/1,610.4	30/20
SWIR-2 (B7/B12)	2,110-2,290/2,202.4/2,185.7	30/20

2.3. Used Indices

The design of spectral water indices takes advantage of the ability of water to absorb energy in near-infrared (NIR) and shortwave infrared (SWIR) wavelengths. Spectral indices like NDWI and MNDWI enhance the contrast between water bodies and surrounding features, making them useful for mapping surface water using satellite imagery. These indices involve combining different spectral bands using mathematical operations, and a threshold value is applied to separate water from other features based on their spectral properties. MNDWI is especially effective at reducing noise from vegetation and soil, as well as in urban areas where there may be a lot of interference. In this study, NDWI and MNDWI indexes were computed using Equation 1 and 2 using Landsat and Sentinel images.

$$NDWI = (Green - NIR)/(Green + NIR) \quad (1)$$

$$MNDWI = (Green - SWIR1)/(Green + SWIR1) \quad (2)$$

where, the green band for Landsat-9 and Sentinel-2 images is represented by B3. The NIR band for Landsat-9 and Sentinel-2 is represented by B5 and B8, respectively. The SWIR band for Landsat-9 and Sentinel-2 is represented by B6 and B11, respectively.

2.4. K-means++ Clustering Algorithm

The k-means clustering algorithm was first suggested by MacQuen (1967) and developed by Lloyd (1982). The k-means clustering method presupposes knowledge of the number of clusters (k) and necessitates initial values for the cluster centers to be seeded to execute. The accuracy of the data assignment to clusters is heavily reliant on the initial seed values. In summary, k-means clustering is considerably influenced by the selection of initial seed values for cluster centers (Agarwal et al., 2012; Khan, 2012). The k-means++ algorithm evaluates the performance of the preliminary seed selection based on the sum of normalized squared differences between the data dimension and the cluster center for a cluster's members (Khan, 2012). In this study, the K-means++ algorithm running on the GEE platform was used (Arthur and Vassilvitskii, 2007). After several trials of different cluster numbers to extract water details via clustering, it was observed that the best result was obtained with three classes, and the cluster number was determined as three. One of the obtained three classes represents the water surface, while the others represent the non-water surface.

2.5. Accuracy Assessment

The accuracy of this study was evaluated using Overall Accuracy (OA), Kappa (κ) statistics, and F1-score. In this study, the Otsu's thresholding method was used to determine water surfaces for NDWI and MNDWI obtained from Sentinel-2 images, and this was used as the basis for evaluating the accuracy in this study (Figure.2). The Otsu thresholding method maximizes the intra-class variance in a bimodal histogram for any image and automatically extract water and non-water surfaces by determining an optimal threshold. This is a widely used technique. (Sekertekin,

2021). An error matrix has been created for accuracy evaluation by considering all pixels (933,337 pixels)

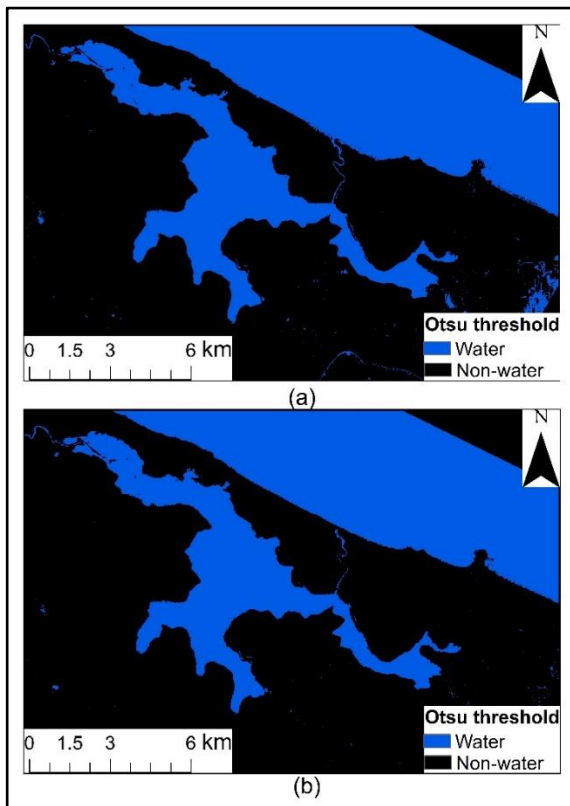


Figure 2. Water surfaces obtained using the Otsu threshold method: a) Sentinel-2 NDWI, b) Sentinel-2 MNDWI

The workflow of this study is shown in Figure 3.

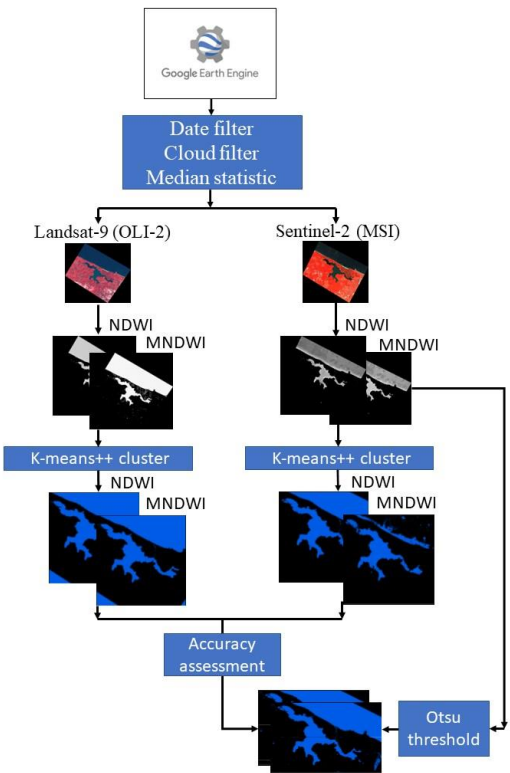


Figure 3. Workflow diagram

3. RESULTS

The accuracy assessment of the Landsat-9 (OLI-2) images used in the study is presented in Table 2 for the images obtained by NDWI, MNDWI, and the K-means++ clustering algorithm, while the images are shown in Figure 4. Overall, accuracy metrics were found to be above 90% based on the obtained using the K-means++ clustering algorithm for both the NDWI and MNDWI. Based on these results, it can be easily said that the K-means++ clustering algorithm utilized to both NDWI and MNDWI indices performed very successfully in extracting water surfaces. The maximum NDWI value obtained from the Landsat-9 image was calculated as 0.855 for water surfaces, while it was +1.000 for MNDWI. The K-means++ algorithm showed higher success in the NDWI image. The NDWI OA and F1-score were calculated as 99.72% and 99.57%, respectively, while these values were calculated as 97.37% and 95.87% in MNDWI. While the F1-score was 99.72% and 99.57%, respectively, these values were calculated as 97.37% and 95.87% in MNDW.

Table 2. Accuracy assessment of the Landsat-9 (OLI-2) images

Indices	OA (%)	κ	F1-score (%)	Area (km ²)
NDWI	99.72	0.994	99.57	29.43
MNDWI	97.37	0.939	95.87	29.45

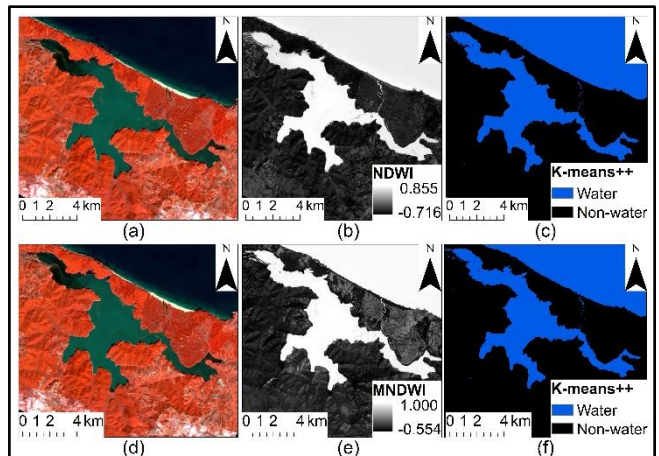


Figure 4. Landsat-9 images where NDWI and K-means++ algorithm were applied: a,d) Landsat-9 false color image, b) Landsat-9 NDWI, c) NDWI K-means++ cluster image, e) Landsat-9 MNDWI, f) MNDWI K-means++ cluster

Accuracy assessment of the Sentinel-2 (MSI) images used in the study is given in Table 3, and the images obtained with NDWI, MNDWI and K-means++ clustering algorithms are shown in Figure 5. The OA obtained with Sentinel-2 images is also calculated to be above 90%. This result shows that water surfaces were successfully detected using NDWI and MNDWI values calculated with Sentinel-2 images in a similar way. The maximum NDWI value obtained from the Sentinel-2 image was calculated as 0.767 for the water surface, while it was calculated as 0.802 for MNDWI. K-means++ algorithm also showed higher performance in the indices obtained from Sentinel-2 images. While the OA and

F1-score of NDWI were calculated as 99.39% and 99.04%, respectively, these values were calculated as 95.26% and 91.99% for MNDW.

Table 3. Accuracy assessment of the Sentinel-2 (MSI) images

Indices	OA (%)	κ	F1-score (%)	Area (km ²)
NDWI	99.39	0.986	99.04	29.08
MNDWI	95.26	0.887	91.99	22.21

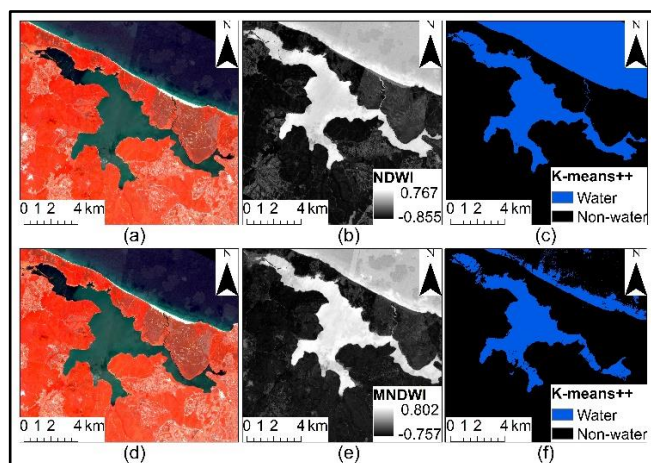


Figure 5. NDWI and K-means++ applied Sentinel-2 (MSI) images: a) Sentinel-2 false color image, b) Sentinel-2 NDWI, c) NDWI K-means++ cluster image, e) Sentinel-2 MNDWI, f) MNDWI K-means++ cluster

4. DISCUSSION AND CONCLUSIONS

Detecting, monitoring, and managing surface waters and water resources is a crucial task for water management. Remote sensing techniques are frequently preferred due to their effectiveness and cost-efficiency when compared to other methods. Recent advancements in satellite imagery, particularly in terms of temporal, spatial, and spectral resolutions, have further increased research in utilizing water surfaces for such tasks. As a result, various methods have been devised to identify water surfaces from satellite imagery.

In this study, water surfaces were extracted from other details using the K-means++ clustering algorithm based on NDWI and MNDWI indices using optical images on the GEE platform. Terkos Lake located within the boundaries of Istanbul province was selected for the study. In the accuracy assessment of the study, Sentinel images with higher resolution than Landsat images were used. Water surfaces were determined using the most preferred Otsu thresholding method for NDWI and MNDWI indices calculated from Sentinel images and used as verification data. The accuracy of the water surfaces obtained with the K-means++ method was evaluated by using all pixels for validation. When the results were evaluated, water surface accuracies obtained through clustering algorithms using both indices were quite successful with OA and F1-score values above 90%. In this study, it was observed that water surfaces obtained using

NDWI were more successful than water surface areas obtained using MNDWI. In many previous studies, many water extraction indices such as NDWI, MNDWI, AWEIsh, AWEInsh, NWI were used (Deng et al., 2020; Guo et al., 2017; Khalid et al., 2021; Rad et al., 2021; Sarp and Ozcelik, 2017; Sunder et al., 2017; Yue et al., 2020; Zhou et al., 2017). Similarly, automatic methods such as Otsu's threshold have been used to distinguish water and land in these indices (Babaei et al., 2021; Cordeiro et al., 2021; Guo et al., 2017; Rad et al., 2021; L. G. de M. Reis et al., 2021; Sekertekin, 2021). However, studies using clustering algorithms are very limited. In this study, water and land separation was easily accomplished using the K-means++ clustering method from NDWI and MNDWI water extraction indices used. Cordeiro et al. (2021) found that the use of clustering algorithms was quite successful in extracting water surfaces. They determined the κ value as 0.874 in their study. When compared with the κ values found in this study, it can be concluded that this study is successful.

This study is promising for automatically detecting water pixels on optical images without the need for auxiliary techniques or pre-trained data using clustering algorithms. However, more research is still needed to address misclassification issues in water surfaces such as clouds, snow, shadows, shallow waters, turbid waters, and green waters.

Ethics Committee Approval

N/A

Peer-review

Externally peer-reviewed.

Author Contributions

All process steps such as conceptualization, investigation, analysis, visualization, methodology and writing were written by Osman Salih Yilmaz. The author has read and agreed to the published version of manuscript.

Conflict of Interest

The authors have no conflicts of interest to declare.

Funding

The authors declared that this study has received no financial support.

REFERENCES

- Agarwal, S., Yadav, S., & Singh, K. (2012). Notice of Violation of IEEE Publication Principles: K-means versus k-means++ clustering technique. In 2012 Students Conference on Engineering and Systems, 1–6.
- Arthur, D., & Vassilvitskii, S. (2007). K-means++: The advantages of careful seeding In: Proceedings of the Eighteenth Annual ACM-SIAM Symposium on Discrete Algorithms. SODA'07, Society for Industrial and Applied Mathematics, 1027–1035, Philadelphia, PA, USA.
- Bayram, B., Seker, D. Z., Acar, U., Yuksel, Y., Guner, H. A. A., & Cetin, I. (2013). An integrated approach to

- temporal monitoring of the shoreline and basin of Terkos Lake. *Journal of Coastal Research*, 29(6), 1427–1435. <https://doi.org/10.2112/JCOASTRES-D-12-00084.1>
- Bouslihim, Y., Kharrou, M. H., Miftah, A., Attou, T., Bouchaou, L., & Chehbouni, A. (2022). Comparing Pan-sharpened Landsat-9 and Sentinel-2 for Land-Use Classification Using Machine Learning Classifiers. *Journal of Geovisualization and Spatial Analysis*, 6(2), 35.
- Cordeiro, M. C. R., Martinez, J. M., & Peña-Luque, S. (2021). Automatic water detection from multidimensional hierarchical clustering for Sentinel-2 images and a comparison with Level 2A processors. *Remote Sensing of Environment*, 253(November 2020). <https://doi.org/10.1016/j.rse.2020.112209>
- Donchyts, G., Schellekens, J., Winsemius, H., Eisemann, E., & van de Giesen, N. (2016). A 30 m resolution surfacewater mask including estimation of positional and thematic differences using landsat 8, SRTM and OpenStreetMap: A case study in the Murray-Darling basin, Australia. *Remote Sensing*, 8(5). <https://doi.org/10.3390/rs8050386>
- Elachi, C., & Van Zyl, J. J. (2021). Introduction to the physics and techniques of remote sensing. John Wiley & Sons.
- Feng, M., Sexton, J. O., Channan, S., & Townshend, J. R. (2016). A global, high-resolution (30-m) inland water body dataset for 2000: first results of a topographic–spectral classification algorithm. *International Journal of Digital Earth*, 9(2), 113–133. <https://doi.org/10.1080/17538947.2015.1026420>
- Feyisa, G. L., Meilby, H., Fensholt, R., & Proud, S. R. (2014). Automated Water Extraction Index: A new technique for surface water mapping using Landsat imagery. *Remote Sensing of Environment*, 140, 23–35. <https://doi.org/10.1016/j.rse.2013.08.029>
- Gao, B.-C. (1996). NDWI—A normalized difference water index for remote sensing of vegetation liquid water from space. *Remote Sensing of Environment*, 58(3), 257–266. [https://doi.org/10.1016/S0034-4257\(96\)00067-3](https://doi.org/10.1016/S0034-4257(96)00067-3)
- Gao, H., Birkett, C., & Lettenmaier, D. P. (2012). Global monitoring of large reservoir storage from satellite remote sensing. *Water Resources Research*, 48(9), 1–12. <https://doi.org/10.1029/2012WR012063>
- Govender, M., Chetty, K., & Bulcock, H. (2007). A review of hyperspectral remote sensing and its application in vegetation and water resource studies. *Water Sa*, 33(2), 145–151.
- Gu, Z., Zhang, Y., & Fan, H. (2021). Mapping inter- and intra-annual dynamics in water surface area of the Tonle Sap Lake with Landsat time-series and water level data. *Journal of Hydrology*, 601(July), 126644. <https://doi.org/10.1016/j.jhydrol.2021.126644>
- Hu, Q., Li, C., Wang, Z., Liu, Y., & Liu, W. (2022). Continuous Monitoring of the Surface Water Area in the Yellow River Basin during 1986–2019 Using Available Landsat Imagery and the Google Earth Engine. *ISPRS International Journal of Geo-Information*, 11(5), 305. <https://doi.org/10.3390/ijgi11050305>
- Ji, L., Zhang, L., & Wylie, B. (2009). Problems of Dynamic NDWI Threshold and Objectives of the Study The NDWI data derived from Landsat MSS, TM, and ETM (Jain et al. *Photogrammetric Engineering & Remote Sensing*, 75(11), 1307–1317. <https://doi.org/10.14358/PERS.75.11.1307>
- Kaya, H., Ertek, T. A., & Gazioglu, C. (2019). Geomorphological Features of Terekos Lake and Surroundings. *International Journal of Environment and Geoinformatics (IJE GEO)*, 6(2), 192–205. <https://doi.org/10.30897/ijegeo>
- Khalid, H. W., Khalil, R. M. Z., & Qureshi, M. A. (2021). Evaluating spectral indices for water bodies extraction in western Tibetan Plateau. *Egyptian Journal of Remote Sensing and Space Science*, 24(3), 619–634. <https://doi.org/10.1016/j.ejrs.2021.09.003>
- Khan, F. (2012). An initial seed selection algorithm for k-means clustering of georeferenced data to improve replicability of cluster assignments for mapping application. *Applied Soft Computing Journal*, 12(11), 3698–3700. <https://doi.org/10.1016/j.asoc.2012.07.021>
- Liu, C., Shi, J., Liu, X., Shi, Z., & Zhu, J. (2020). Subpixel mapping of surfacewater in the Tibetan Plateau with MODIS data. *Remote Sensing*, 12(7), 1–20. <https://doi.org/10.3390/rs12071154>
- Lloyd, S. (1982). Least squares quantization in PCM. *IEEE Transactions on Information Theory*, 28(2), 129–137.
- MacQuen, J. B. (1967). Some methods for classification and analysis of multivariate observation. *Proceedings of the 5th Berkley Symposium on Mathematical Statistics and Probability*, 281–297.
- Mahdianpari, M., Salehi, B., Mohammadimanesh, F., & Motagh, M. (2017). Random forest wetland classification using ALOS-2 L-band, RADARSAT-2 C-band, and TerraSAR-X imagery. *ISPRS Journal of Photogrammetry and Remote Sensing*, 130, 13–31. <https://doi.org/10.1016/j.isprsjprs.2017.05.010>
- Maktav, D., Sunar Erbek, F., & Kabdasli, S. (2002). Monitoring coastal erosion at the Black Sea coasts in Turkey using satellite data: A case study at the Lake Terekos, North-west Istanbul. *International Journal of Remote Sensing*, 23(19), 4115–4124. <https://doi.org/10.1080/01431160110115979>
- Mansaray, L. R., Wang, F., Huang, J., & Yang, L. (2019). Accuracies of support vector machine (SVM) and random forest (RF) in rice mapping with Sentinel-1A, Landsat-8 and Sentinel-2A datasets. *Geocarto International*, 0(0), 1–17. <https://doi.org/10.1080/10106049.2019.1568586>
- McFeeters. (1996). The use of the Normalized Difference Water IndexMcFeeters. *International Journal of*

- Remote Sensing, 17(7), 1425–1432.
<https://doi.org/10.1080/01431169608948714>
- McFeeters, S. K. (2013). Using the normalized difference water index (ndwi) within a geographic information system to detect swimming pools for mosquito abatement: A practical approach. *Remote Sensing*, 5(7), 3544–3561. <https://doi.org/10.3390/rs5073544>
- Nguyen, U. N. T., Pham, L. T. H., & Dang, T. D. (2019). An automatic water detection approach using Landsat 8 OLI and Google Earth Engine cloud computing to map lakes and reservoirs in New Zealand. *Environmental Monitoring and Assessment*, 191(4), 1–12. <https://doi.org/10.1007/s10661-019-7355-x>
- Owusu, C. (2022). PyGEE-SWToolbox : A Python Jupyter Notebook Toolbox for Interactive Surface Water Mapping and Analysis Using Google Earth Engine. *Sustainability*, 14, 2557.
- Pekel, J. F., Cottam, A., Gorelick, N., & Belward, A. S. (2016). High-resolution mapping of global surface water and its long-term changes. *Nature*, 540(7633), 418–422. <https://doi.org/10.1038/nature20584>
- Qiao, C., Luo, J., Sheng, Y., Shen, Z., Zhu, Z., & Ming, D. (2012). An Adaptive Water Extraction Method from Remote Sensing Image Based on NDWI. *Journal of the Indian Society of Remote Sensing*, 40(3), 421–433. <https://doi.org/10.1007/s12524-011-0162-7>
- Rad, A. M., Kreitler, J., & Sadegh, M. (2021). Augmented Normalized Difference Water Index for improved surface water monitoring. *Environmental Modelling and Software*, 140(March), 105030. <https://doi.org/10.1016/j.envsoft.2021.105030>
- Reis, S., & Yilmaz, H. M. (2008). Temporal monitoring of water level changes in Seyfe Lake using remote sensing. *Hydrological Processes*, 22(22), 4448–4454. <https://doi.org/10.1002/hyp.7047>
- Sekertekin, A. (2021). A Survey on Global Thresholding Methods for Mapping Open Water Body Using Sentinel-2 Satellite Imagery and Normalized Difference Water Index. *Archives of Computational Methods in Engineering*, 28(3), 1335–1347. <https://doi.org/10.1007/s11831-020-09416-2>
- Tang, H., Lu, S., Baig, M. H. A., Li, M., Fang, C., & Wang, Y. (2022). Large-Scale Surface Water Mapping Based on Landsat and Sentinel-1 Images. *Water* (Switzerland), 14(9). <https://doi.org/10.3390/w14091454>
- Xu, H. (2006). Modification of normalised difference water index (NDWI) to enhance open water features in remotely sensed imagery. *International Journal of Remote Sensing*, 27(14), 3025–3033. <https://doi.org/10.1080/01431160600589179>
- Yang, X., Zhao, S., Qin, X., Zhao, N., & Liang, L. (2017). Mapping of urban surface water bodies from sentinel-2 MSI imagery at 10 m resolution via NDWI-based image sharpening. *Remote Sensing*, 9(6), 1–19. <https://doi.org/10.3390/rs9060596>
- Yilmaz, O. S. (2023). Spatiotemporal statistical analysis of water area changes with climatic variables using Google Earth Engine for Lakes Region in Türkiye. *Environmental Monitoring and Assessment*, 195(6), 735. <https://doi.org/10.1007/s10661-023-11327-1>
- Yilmaz, O. S., Gulgen, F., Balik Sanli, F., & Ates, A. M. (2023). The Performance Analysis of Different Water Indices and Algorithms Using Sentinel-2 and Landsat-8 Images in Determining Water Surface: Demirkopru Dam Case Study. *Arabian Journal for Science and Engineering*, 48, 7883–7903. <https://doi.org/10.1007/s13369-022-07583-x>
- Zhang, Y., Liu, X., Zhang, Y., Ling, X., & Huang, X. (2018). Automatic and unsupervised water body extraction based on spectral-spatial features using GF-1 satellite imagery. *IEEE Geoscience and Remote Sensing Letters*, 16(6), 927–931.